Genetic approach to synaptic biology: synaptic targeting and functional imaging of synapse

Fei Zhu

Supervisor: Prof. Seth Grant

Second Supervisor: Dr. Leon Lagnado

Abstract

In mammalian brain, the postsynaptic density (PSD) is an electron-densed structure in the postsynaptic compartment of excitatory synapses. Proteomics approaches have begun to unravel the molecular composition of PSD complex and discovered a remarkable degree of complexity. Among them, four major components from a scaffolding MAGUKs family (membrane associated guanylate kinase), including PSD-95, PSD-93, SAP-102 and SAP-97, were identified. The MAGUK proteins assemble the NMDA receptor signaling complex, thus play a key role in synaptic strengthening. Previous studies have shown that individual MAGUK protein has different expression pattern in various brain regions. Different MAGUK proteins are also found to regulate the trafficking of distinct neurotransmittor receptor subtypes at different developmental stages, suggesting a high molecular diversity in neuronal cells existing in both spatial and temporal dimensions. However, whether this molecular heterogeneity exists in individual synapse is still not clear. In my PhD, I will utilize integrated approaches including gene targeting, ES cell engineering, functional imaging and RNAi-mediated knock-down to understand the molecular heterogeneity and functional dynamics of individual synapses. In the first stage of my project, I have generated PSD95-EGFP and Arc-Venus knockin ES cell lines, in which fluorescent protein coding sequence (EGFP and Venus) was inserted into the C-terminus of gene of interest (PSD-95 and Arc). I next performed an *in vitro* differentiation of PSD95-EGFP targeted ES cells into neurons (ESNs). My preliminary results showed that PSD95-EGFP fusion protein in ESNs is localized to the postsynaptic side of excitatory synapses, suggesting that inserting the EGFP tag into PSD-95 did not alter the expression and localization of endogenous protein, thus confirm my experimental frame-work. Moreover, the immunostaining results of PSD95-GFP/SAP-102 and PSD95-EGFP/GluR1 showed that their co-localization pattern only appeared in a proportion of synapses, suggesting that a molecular heterogeneity may exist at individual synaptic level.

My next step is to continue generating constructs of which MAGUK genes fused with different fluorescent tags (PSD93-mCER and SAP102-mKO). To address the synaptic heterogeneity question, I intend to perform a second round of gene targeting to tag a different gene locus in those engineered ES cells. After inducing differentiation of these double targeted ESNs, I will characterize the subcellular localization and dynamics of tagged molecules within individual synapses *in vitro* by employing various imaging techniques (i.e. FRAP and real-time imaging) combined with pharmacological treatment and RNAi experiment. In the long-term, I aim to complete the generation of three MAGUKs and Arc gene knock-in mice (PSD95-EGFP, PSD93-mCER, SAP102-mKO and Arc-Venus). These fluorescently tagged mice will also be used to generate double knock-in mice (i.e. PSD95-EGFP mice and SAP102-mKO mice) in which multiple tagged synaptic proteins can be observed simultaneously.

Introduction

In mammalian brain, millions of neurons assemble a massive network of circuitry for processing information. These neurons communicate with each other via a specialized contact structure between the pre-synaptic axon and postsynaptic compartment, termed as the synapse. Under the electron microscopy, a synapse is characterized by a thickening of the postsynaptic membrane called postsynaptic density (PSD) (Figure 1). Although it appears that all synapses share a few core components, at least some of the apparent molecular diversity in receptors and scaffold proteins in the PSD, reflects the fact that individual synapses are heterogeneous. And this synaptic heterogeneity can be seen in a spatial (anatomical) and temporal (developmental) manner. Considering only one single synapse, a heterogeneous molecular feature within synapse, in large part determined by neural activity changes, also exists (Figure 2). Thus, by modifying the strength of synaptic response at individual synapses, the mammalian brain possesses a high degree of cognitive complexity.

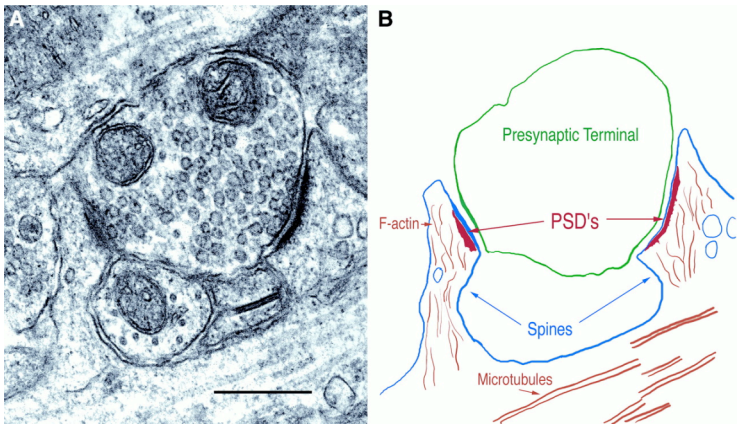

Figure 1. (A) Electron-microscopic picture of synapses. A presynaptic terminal forming synapses with two dendritic spines. (B) Tracing of (A), identifying major synaptic structures. Spines contain an actin-enriched cytoskeleton and PSD lying underneath the postsynaptic membrane (Kennedy 2000).

Consistent with the proposed model of heterogeneity, evolutionary analysis of the PSD proteome suggests that there has been a great molecular expansion in the mammalian PSD compared to that of lower organisms. Mammals not only have a larger number of molecules at postsynaptic site, their potential combinations to form various complexes also greatly increased, thus suggesting an immense molecular diversity is evolved in higher organisms to correlate with more complex cognitive function of the brain (Emes, Pocklington et al. 2008).

In particular, the authors found that the scaffolding protein family MAGUKs (membrane associated guanylate kinase proteins) showed substantial molecular expansion from invertebrate (fly) to vertebrate (mouse).

Early proteomic studies have identified one of the most abundant components of the PSD, PSD-95, as a major member of MAGUKs family. Other MAGUK members including PSD-93, SAP-102 (Synapse associated protein) and SAP-97 were also subsequently identified (Brenman, Christopherson et al. 1996; Kim, Cho et al. 1996; Muller, Kistner et al. 1996).

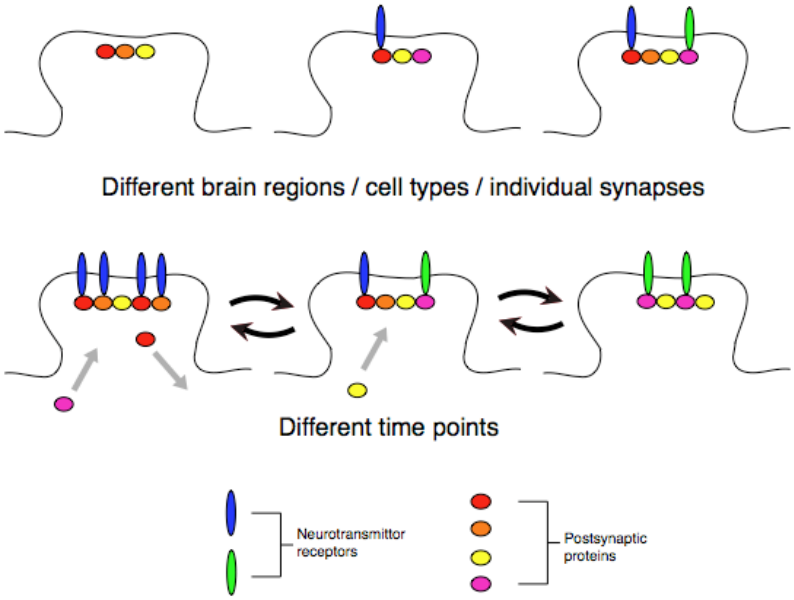

Figure 2. Proposed model of molecular heterogeneity of synapses.

All MAGUKs share a common structural organization including three N-terminal PDZ (PSD-95/Discs large/Zona occluden-1) domains followed by an SH3 (Src-homology 3) domain and a C-terminal apparently enzymatically inactive guanylate kinase (GK) domain (Figure 2). It has been found that the palmitoylation sequence on the N-terminus is critical for targeting PSD-95 to the postsynaptic density. The first and second PDZ domains of MAGUKs bind specifically to the C-terminal tails of NMDA receptor type-2 (NR2) subunit (Kornau, Schenker et al. 1995; Niethammer, Kim et al. 1996) and cluster them on the membrane surface. Thus MAGUKs and PSD-95 in particular are closely coupled to the glutamate receptors, ion channels and other structural and signaling molecules to organize the assembly of NMDA receptor signaling complex. On the other hand, it has been reported that PSD-95 also determines the membrane density of AMPA receptors through its direct binding

with Stargazin, a TARP (transmembrane AMPAR regulatory proteins) family member which interacts directly with AMPA receptor (Schnell, Sizemore et al. 2002). Therefore, by controlling the trafficking and subcellular localization of different glutamate receptors, the MAGUKs play key roles in the regulation of synaptic architecture.

Although all MAGUK members express widely through out the mammalian brain, it has been found that their relative abundance in specific brain region is different. For example, PSD-95, SAP-102 and PSD-93 mRNA were all highly expressed in the telecephalon and the pyramidal cell layer of the hippocampus displayed the highest expression. PSD-95 and SAP-102 mRNA were also detected in the cerebeller cortex, with low to moderate signals in the thalamic and brainstem regions. By contrast, PSD-93 mRNA expressed at moderate levels in the Purkinje cell layer of the cerebellum, and weakly were detected in the thalamus (Fukaya, Ueda et al. 1999). Consistent with the mRNA expression data, MAGUK proteins also showed distinct expression patterns among various brain regions. In addition to their different spatial distribution in various brain regions, the MAGUKs also display distinct expression levels at different developmental stages. In rat hippocampus, SAP-102 expression is high during late

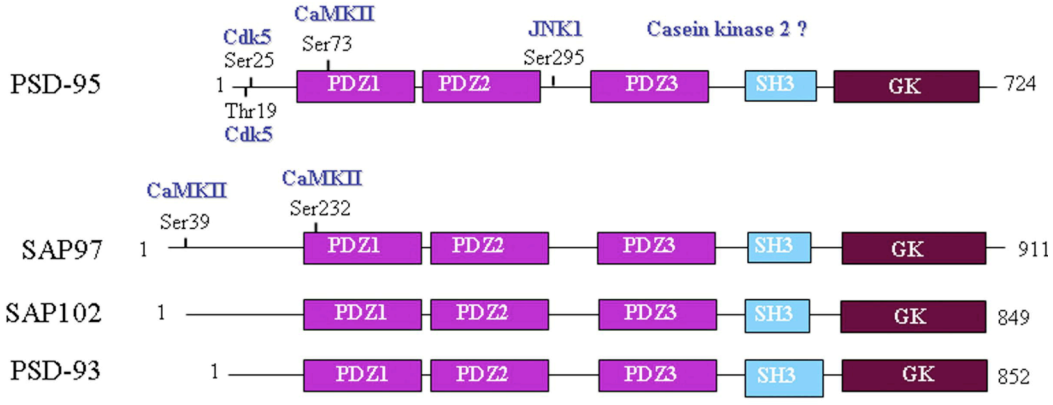

Figure 3. Schematic view of domain structures of PSD-MAGUK protein family. PDZ, PSD-95/Disc large/Zona occluden-1 domain; SH3, src-homology 3 domain; GK, guanylate kinase domain (Gardoni, Marcello et al. 2009).

embryonic development and early postnatal life, and decreases with age, whereas PSD-95 and PSD-93 are weakly expressed during early postnatal life but increase significantly by the age of one month (Sans, Petralia et al. 2000). Moreover, comparing PSD-95, PSD-93 and SAP-102 knock-out (KO) mice revealed distinct synaptic plasticity phenotypes in responses to different patterns of neural stimuli in hippocampal synapses; behavioral tests of these KO

mice also suggested unique cognitive phenotypes in learning and memory tasks for each mutant, implying that a certain degree of functional heterogeneity of MAGUK. Indeed, a recent study has shown that different MAGUKs regulate the trafficking of various glutamate receptor subtypes during synapse development (Elias, Elias et al. 2008), which suggests that heterogeneous features of individual synapses may be derived from the selective trafficking of receptors by different MAGUKs.

It has been well known that the morphology and strength of synapses is highly dynamic, not only during the developmental stages but also in response to neural activity changes such as long-term potentiation (LTP) and long-term depression (LTD). In glutamatergic synapses, persistent stimulation of various forms of LTP or LTD is dependent upon rapid gene expressions. The activity-regulated immediate early genes (IEGs) have been widely studied and implicated in this process (Sheng and Greenberg 1990). In particular, substantial research has been focused on the IEG gene termed Arc/Arg 3.1 (activity-regulated cytoskeleton-associated protein). Arc/Arg3.1 is found in the PSD, co-immunoprecipitated with the NMDA receptor complex (Husi, Ward et al. 2000). Once activated by patterned synaptic activity, including natural stimuli, seizure, LTP and memory-related behavioral experience, newly synthesized Arc mRNA rapidly traffics to the dendrites and selectively accumulates at activated synapses (Steward and Worley 2001). Most interestingly, Arc protein also localizes to and becomes enriched at the local synapse that had been stimulated, suggesting that Arc protein is locally synthesized (Yin, Edelman et al. 2002; Moga, Calhoun et al. 2004). The induction of Arc including its mRNA transport, translation and the local protein synthesis all depend on the activation of NMDA receptors as well as the MAPK/ERK signaling cascade (Waltereit, Dammermann et al. 2001). Newly translated Arc functions to regulate AMPA receptors trafficking. Using the yeast two hybrid system, one recent study has shown that Arc interacts with dynamin and specific isoforms of endophilin, and modulates AMPA receptor trafficking by accelerating endocytosis and reducing its surface expression (Chowdhury, Shepherd et al. 2006). Consistent with these findings, Arc knockout mice exhibit significantly impaired long-term depression together with a biphasic alteration of LTP in the hippocampal neurons, and these animals fail to form long-lasting memories for implicit

and explicit learning tasks (Plath, Ohana et al. 2006). Although it has been clear that Arc binds endophilin and dynamin, the molecular mechanism of how this complex induces selective trafficking of AMPAR remain unknown, since the Arc complex does not directly bind AMPA receptor (AMPAR) directly. Biochemical analysis of the PSD complex using Arc-TAP knockin mice revealed that Arc protein specifically and physically interacts with PSD-95 in vivo (unpublished data, Fernandes E.). Thus, it is reasonable to hypothesize that PSD-95 plays a pivotal role during the Arc-mediated AMPAR trafficking (Figure 4).

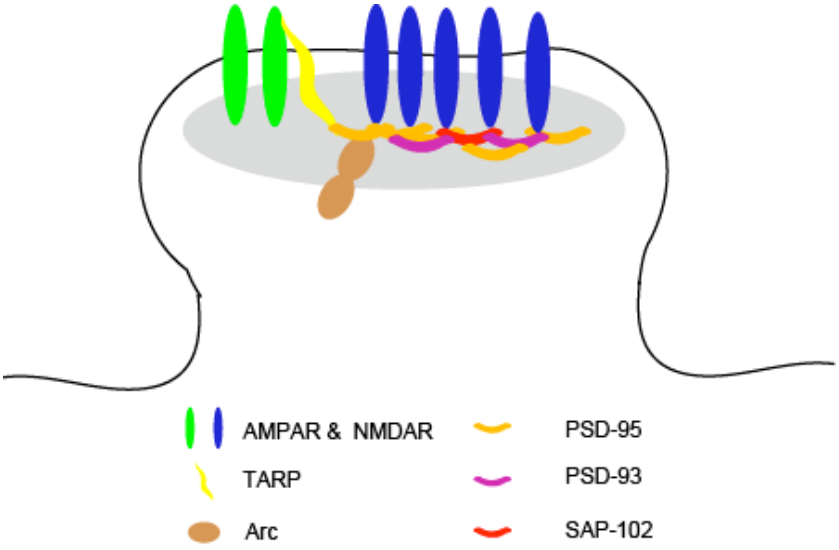

Figure 4. Proposed molecular interactions for Arc modulating AMPA trafficking. The complex of Arc, endophilin and dynamin modulates AMPA receptors endocytosis and its surface density on the membrane. Recent studies implicated that PSD-95 may play a key role during the Arc-mediated AMPA receptor (AMPAR) trafficking.

Despite advances in our understanding of the molecular composition of the PSD-MAGUKs as well as Arc in spine synapse, the full extent of synaptic heterogeneity is still unknown. Questions such as whether this heterogeneity, which may be derived from the molecular diversity of MAGUKs, exists in single synapse; how this synaptic heterogeneity is established and maintained in response to synaptic plasticity; what is the cellular and molecular mechanism that determine the synaptic heterogeneity still remain to be answered.

Project Aim

The broad aim of my project is to understand the molecular heterogeneity and functional dynamics of individual synapses.

To do that, I will first insert different fluorescent protein coding sequences (Venus, EGFP, mCER and mKO) in-frame into the C-terminus of each of the candidate genes (Arc, PSD-95, PSD-93 and SAP-102) to generate ES cells that carry the fluorescent tags (Arc-Venus, PSD95-EGFP, PSD93-mCER and SAP102-mKO). Taking advantage of the gene targeting approach for tagging at C-terminal of candidate genes established in our lab (Fernandes E. et al., unpublished data), I will be able to repeatedly swap various fluorescent tags that are in-frame and fused with the genes of interest. After establishing targeted ES clones, I will characterize the fusion protein expression in these ES cells derived neurons (ESNs) *in vitro* by applying a well-established differentiation protocol (Fernandes E., unpublished data). Functional analysis to investigate the molecular diversity of individual synapses in these cultured neurons will be carried out employing various fluorescent-imaging techniques. The long-term goal of this project is to generate various fluorescent-tagged Arc and MAGUK gene knockin mice and study the synaptic heterogeneity and dynamics.

Methods and Materials

PCR Amplification

The EGFP and Venus coding sequences flanked with restriction enzyme recognition sites were amplified using the following designed primers:

Forward: 5’ cggcgctctagaggtggcggtagtatggtgagcaagggcgaggagctg 3’

Reverse: 5’ ctcggcatggacgagctgtacaagtgatgatcaacggtt 3’

The amplification reactions were carried out using Expand Long Template PCR system (Roche, Cat no. 11681842001). PCR reaction was performed for 25 cycles, consisting of 2 min at 94°C, 30 second at 65°C and 150 second at 68°C. PCR products were resolved on 2% agarose gel and confirmed by enzyme digestion and sequencing.

Recombineering in *E.coli*

The recombineering procedure was essentially the same as described previously (Liu, Jenkins et al. 2003). *E. coli* EL350 harboring the recipient plasmid were grown at 32°C to an optical density (OD) 600 nm = ~0.5 in Luria-Bertani Medium (LB) in the presence of tetracycline. The cells were then shifted to 42°C for 15 min shaking at 220 rpm to induce the λ phage genes (*exo*, *bet* and *gam*) expression, followed by chilling on wet ice for 10 min. Electro-competent cells were prepared by washing the cells three times with ice-cold water. About 150 ng of purified DNA fragments were electroporated into ~50 μg of ice-cold electro-competent cells. After electroporation, 1 ml of LB medium was added immediately to the cuvette. The culture was incubated at 32°C for 1 hour with shaking before spreading on selective LB plate.

ES cell culture

Murine ES cell line E14 TG2a were maintained on gelatine-coated plastic multiple well plates or Petri-dishes in ES media containing GMEM (Glascow's Modified Eagle's Medium), 10% ES-culture serum (Stem Cell Tech), 1% nonessential amino acid, 1% sodium pyruvate, 2 mM L-glutamine, 100 μM 2-mercaptoethanol and supplemented with 1000 U/ml leukemia inhibitory factor (LIF) (Chemicon) at 37°C in humidified air with 5% CO_2. All cell culture reagents were purchased from Invitrogen unless otherwise specified.

Gene targeting in ES cells

One hundred microgram of targeting vector (pTARGETER-PSD95EGFP, pTARGETER-ArcVenus) DNA linearized by PvuI was electroporated into $1x10^7$ mouse E14 ES cells. After transfection, cells were grown with ES medium supplemented with 500 μg/ml G418. Surviving colonies obtained from drug selection were picked, expanded and frozen. Genomic DNA from these clones was extracted and analyzed by long range PCR to identify correct targeted clones.

In vitro differentiation of ES cells derived neurons

In vitro differentiation of ES cells derived neurons was performed according to a

well-established protocol in our lab based on the previous publication (Stavridis and Smith 2003). Wild type and PSD95-EGFP targeted ES cells were grown on gelatin-coated T25 flasks in normal ES media. After becoming fully confluent, ES cells were trypsinized and transferred to bacterial dishes allowing the formation of embryoid bodies (EB). EBs were maintained for 3 days in the absence of leukaemia inhibitory factor (LIF) and subsequently plated on new dishes with media supplemented with 10 μl/ml retinoic acid. After 5 days, cells were trypsinized, titrated to a single-cell suspension and seeded on laminin-coated Petri-dishes or coverslips in the overnight plating media containing equal amount of DMEM and F12 Ham (Invitrogen) supplemented with 1% B27 and 0.1% FGF. On the following day, the media was replaced with neurobasal media supplemented with 0.5% L-glutamine and 2% B27.

Immunocytochemistry and Image acquisition

Wild type and PSD95-EGFP expressing neurons were fixed with chilled (-20°C) methanol for 7 min and blocked with PBS containing 10% bovine serum albumin, 0.2% Triton X-100 and incubated with the following primary antibodies: anti-GFP (1:200, Invitrogen), synaptophysin (1:1000, Chemicon), MAP2B (1:200, Abcam), SAP-102 (1:100, Santa Cruz) and GluR1 (1:100, Chemicon), followed by cyanine 3-, cyanine 2-, and cyanine 5- conjugated secondary antibodies (Jackson Immunoresearch Laboratories). Fluorescent images were acquired using a Zeiss LSM 510-META laser scanning confocal microscope with 40x or 63x Plan-Apochromat objectives.

Results

Generation of PSD95-EGFP targeted ES cells.

Based on available template vectors in our lab (kindly provided by Fernandes E.) which contain PSD-95 mini homology arms (PCR amplified using a BAC library derived from mouse ES clones AB2.2 corresponding to the mouse strain 129S7), I prepared a targeting vector in which EGFP coding sequence was inserted into the open reading frame of PSD-95 gene on 3' end and immediately before the stop codon of exon 19 (Figure 5A).

EGFP fluorescent tag was first amplified by PCR using designed primers. The 5'-end tail of forward primers contains an *Xba*I site followed by additional linker sequences coded for 4 amino acids (Gly-Gly-Gly-Ser), whereas the 5'-end tail of reverse primers contains a *Bcl*I restriction site. The ~700 bp PCR products were directionally cloned into the p*neoflox* vector which already contains PSD-95 mini homology arms, the PGK EM7 promoter sequences, *Neo*^{r} gene and a SV40 polyadenylation site flanked by two *lox*P sites. The PGK EM7-*Neo*^{r} genes allow for G418 selection of ES cells after electroporation. The *neo* cassette is flanked by two *lox*P sites, thus allowing Cre-mediated removal. The DNA fragment flanked by these two mini homology arms was excised and transformed into *E.coli* EL350 harboring the recipient vector pTargeter, which contains the genomic sequence of PSD-95. By homologous recombination, the EGFP gene together with PGK EM7-*lox*P-*neo*^{r}-*lox*P-SV40pA cassette was inserted into the pTargeter vector. The final targeting vector contains a 5' end homology arm of ~6.3 kb and a 3' end homology arm of ~2.9 kb. This recombination event resulted in a fusion protein that consists of three PDZ domains, an SH3 domain, a guanylate kinase (GK) domain and EGFP (Figure 5B).

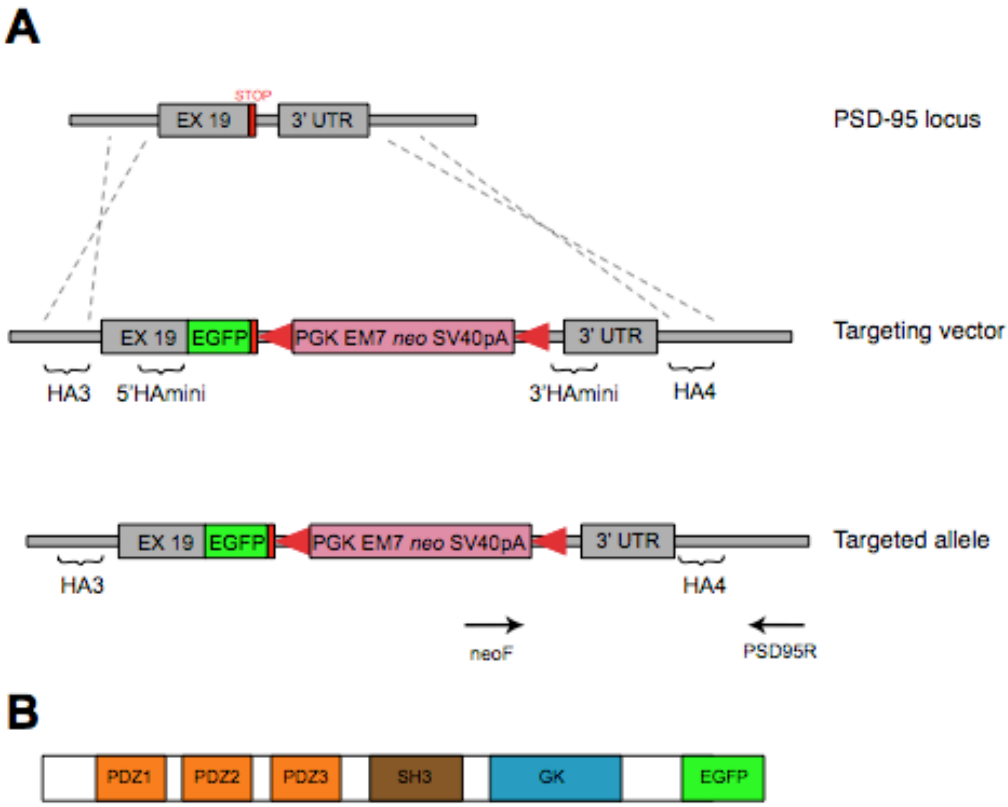

Figure 5. Generation of PSD95-EGFP targeted allele in ES cells. (A) Scheme of the targeted genomic PSD-95 locus. The PSD-95 allele was targeted by inserting EGFP coding sequence into the 3' end of exon 19. Red thick lane: stop codon of the coding sequence; Triangle: *lox*P sites. (B) Schematic view of PSD-95 protein containing three PDZ domains, an SH3 domain and a GK domain C-terminally fused with EGFP.

The targeting vector was linearized by PvuI enzymatic digestion and subsequently electroporated into mouse E14 ES cells. G418 selection was performed for 8-10 days, two hundred and fifty eight *Neo*^{r} colonies were picked, expanded and frozen. Genomic DNA from these colonies was exacted and analyzed by long range PCR genotyping using designed primers with specificity for the *Neo*^{r} gene and PSD-95 genomic sequence outside the 5' homology arm (Figure 5A). Two positive ES clones showing the band with expected size of 3388 bp were identified (Figure 6). One positive PSD95-EGFP ES clone was then injected into the blastocysts. Five agouti chimeric male mice were generated.

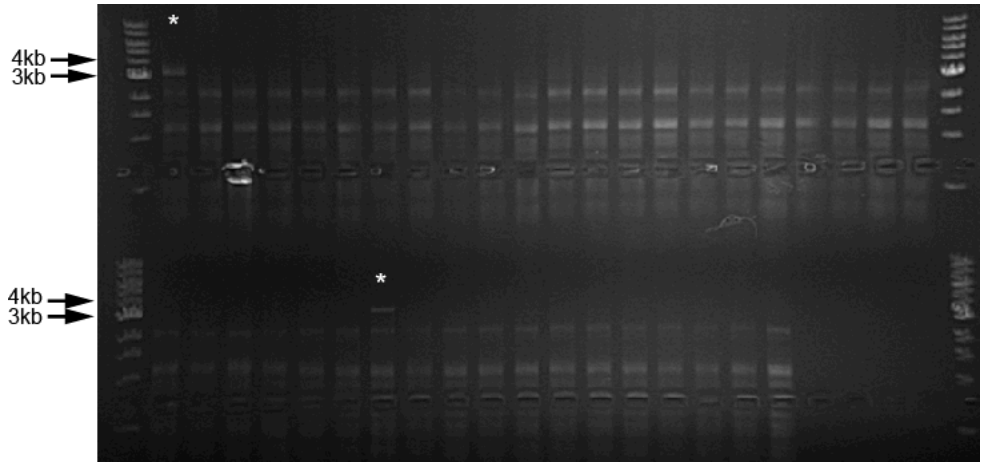

Figure 6. Analysis of PSD95-EGFP targeted ES cells using polymerase chain reaction genotyping. Most of the clones showed unspecific amplified product, whereas two positive clones (lanes marked with aster) showed expected3388-bp bands.

In vitro differentiation of PSD-95-GFP targeted ES cell derived neurons (ESN).

Using a standard recombineering technique, I have generated PSD95-EGFP fusion construct and established PSD95-EGFP targeted ES clones. Previous studies have shown that PSD-95 expression is low during early postnatal life but greatly increased with age, implying PSD-95 is preferentially expressed in mature neurons (Sans, Petralia et al. 2000). To further examine the cellular expression level of PSD95-EGFP fusion protein, I performed an *in vitro* assay to generate neurons that are differentiated from ES cells according to a well-established protocol in our lab (see Methods and Materials), which yields highly enriched neurons.

Wildtype (WT) and PSD95-EGFP targeted E14 cells were cultured and induced to differentiate into neurons *in vitro* as described above. Live cell fluorescent images were taken at different time interval after differentiation induction. I found that, at 13 day *in vitro*, cells growing in neuronal differentiation medium displayed typical neuronal cell morphology, whereas no EGFP fluorescence was observed. At 21 days *in vitro*, cells showed occasional EGFP-positive punctuate structures with weak green fluorescence intensity, whereas after 39 days growing *in vitro*, those neurons showed significantly increased level of EGFP fluorescence as monitored by visual inspection (Figure 7). Although a quantitative microscopic measurement of the EGFP fluorescent intensity are yet required to further validate the above observations, my results demonstrate that the targeted ESNs start to have stable and robust expression of PSD95-EGFP protein at approximately 21 days after

differentiation. These data are consistent with the previous studies (Okabe, Kim et al. 1999; Marrs, Green et al. 2001), suggesting that tagging of PSD-95 with EGFP does not alter the cellular expression pattern of the endogenous protein in neurons.

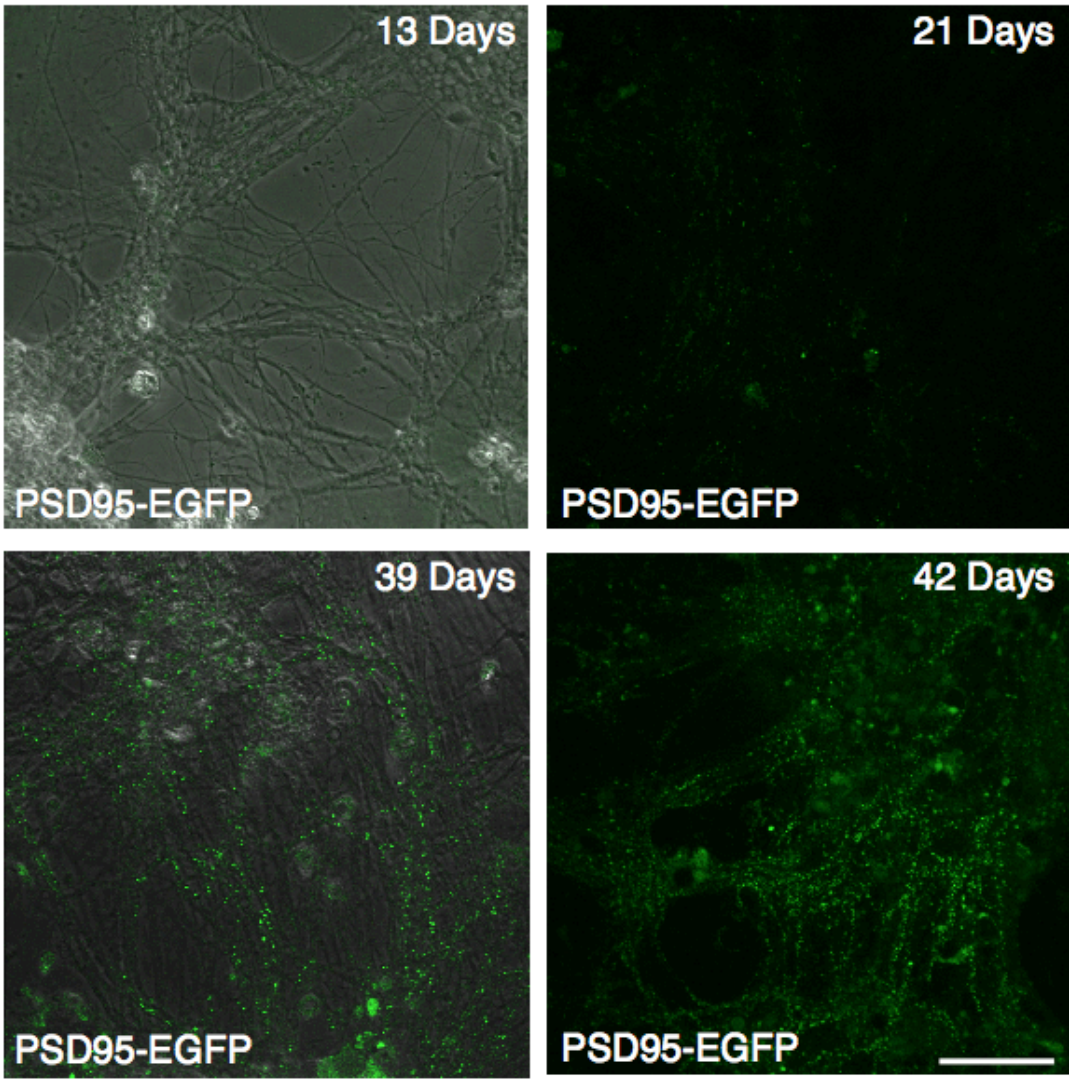

Figure 7. Expression of PSD95-EGFP in ES cells derived neurons (ESNs). The EGFP fluorescent images are superimposed onto the transmitted confocal images (upper and bottom left panels). All green fluorescence shown in figures are images from direct detection of EGFP signals. At 13 days, cells growing in *in vitro* displayed typical neuronal cell morphology, whereas no green fluorescence was detected (upper left panel). At 21 days after differentiation, occasional EGFP-positive punctuates can be detected in the cultured ESNs (upper right panel), whereas after 39 days growing *in vitro*, these ESNs showed greatly increased level of EGFP fluorescence (bottom panel). Scale bar: 25 μm.

Postsynaptic localization of PSD95-EGFP

To test the fluorescent punctum structure observed from engineered ESNs could accurately reflect the postsynaptic localization of PSD95-EGFP fusion protein, I performed

immunocytochemistry experiment using 33 days-old *in vitro* differentiated PSD95-EGFP ESNs. Cultured neurons were fixed and stained with anti-GFP antibody. As shown in Figure 8A and 8B, the specific subcellular distribution of PSD95-EGFP to the postsynaptic component can be examined by using the pre-synaptic marker, anti-Synaptophysin and dendritic marker, anti-MAP2 antibodies. I found that the discrete, bright PSD95-EGFP puncta, which were absent from control WT cells (Figure 8A), appeared on the somata and processes that were immunoreactive for MAP2 (Figure 8B). In addition, I observed that the majority of pre-synaptic terminals labeled by synaptophysin staining were in close apposition to PSD95-EGFP immunoreactive puncta (Figure 8B inset). Taken together, these results suggest that PSD95-EGFGP puncta localize to the sites opposing to the pre-synaptic terminals.

To further confirm the subcellular localization of PSD95-EGFP in the postsynaptic sites, I next carried out immunostaining experiments using GluR1 and SAP-102 antibodies that are known to localize at postsynaptic side of synapses. Consistent with the staining pattern by using antibody against endogenous PSD-95 in WT ESNs (data not shown), most of the PSD95-EGFP puncta colocalize with SAP-102 immunoreactive staining (Figure 8C inset, arrowheads), suggesting that PSD95-EGFP is localized to the postsynaptic sites. Similar to GFP and SAP-102 staining pattern, dual labeling with GFP and GluR1 antibodies also displayed their colocalization within most of the synapses (Figure 8D inset, arrowhead). In summary, these data confirm that PSD95-EGFP is localized to the postsynaptic side of synapses and demonstrate that inserting EGFP tag into PSD-95 did not alter the postsynaptic localization of endogenous protein. Therefore, the PSD95-EGFP fusion protein may be used as a reliable PSD marker in synapses.

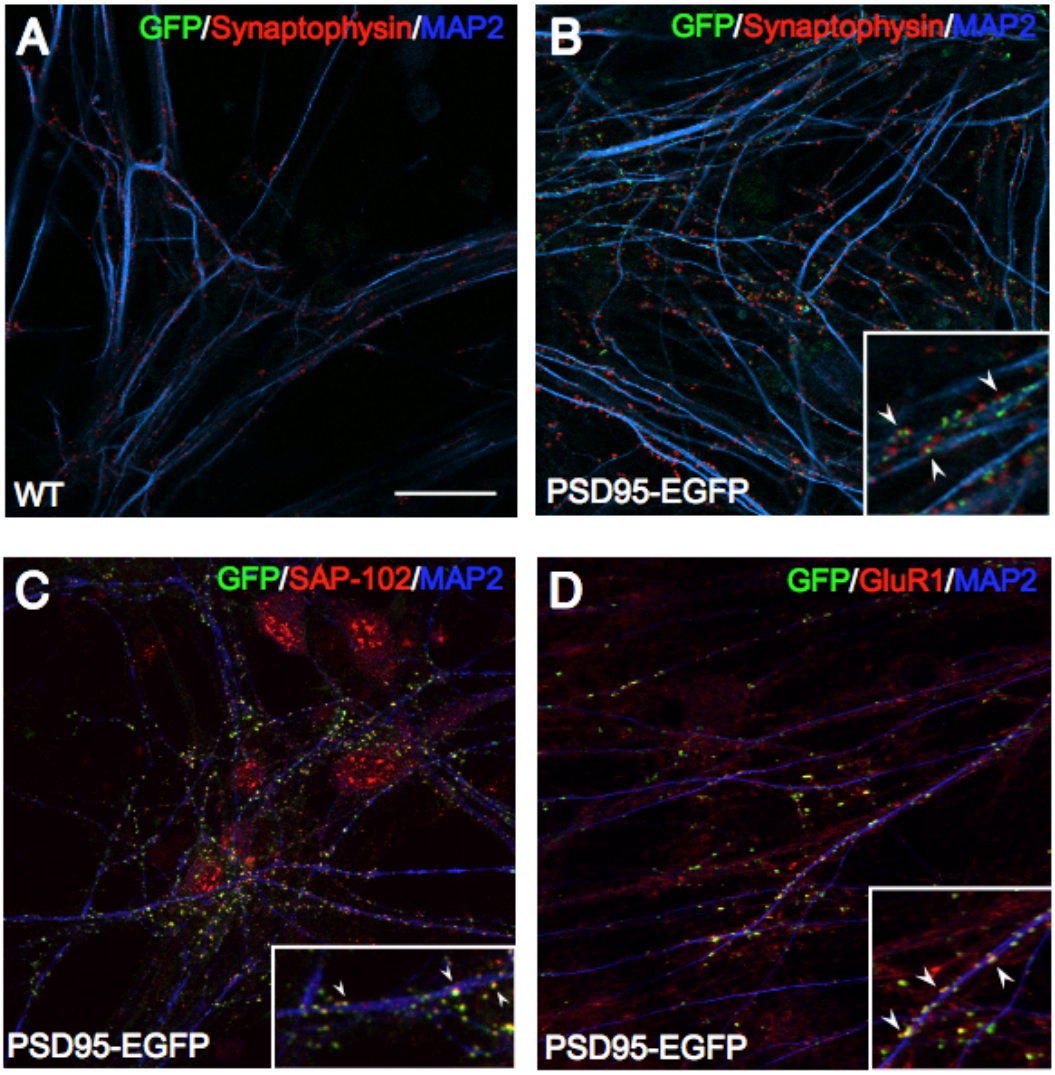

Figure 8. Postsynaptic localization of PSD95-EGFP in ESNs. (A and B) Wildtype and PSD95-EGFP ESNs are immunostained with anti-GFP (green), anti-Synaptophysin (red) and anti-MAP2 (blue) antibodies. (A) In wildtype ESNs, no GFP staining was observed. (B) In PSD95-EGFP expressing ESNs, the synaptophysin staining puncta are in close apposition with GFP-positive puncta (inset, arrowhead). (C) Image shows cultured PSD95-EGFP ESNs stained with anti-GFP (green), anti-SAP-102 (red) and anti-MAP2(blue) antibodies. Arrowheads in the boxed region showed that GFP-immunoreactive puncta are colocalized with SAP-102 staining. (D) PSD95-EGFP ESNs are visualized by immunofluorescence staining using antibodies again GFP(green), GluR1(red) and MAP2(blue). Arrowheads in insets showed GFP staining colocalizes with GluR1-positive puncta structure. Note that in panel (C)and (D), colocalization of PSD95-EGFP with SAP-102 or GluR1 only appears in a fraction of synapses. Insets are four times of magnification of the images. Scale bar: 20 μm.

Generation of Arc-Venus targeted ES cells

By applying a strategy similar to the generation of PSD95-EGFP targeted ES cells, I have developed Arc-Venus knockin ES clones. The coding sequence of fluorescent tag Venus was in-frame inserted in-frame into the 3' end of endogenous Arc gene through homologous

recombination in ES cells. After G418 selection, two hundred and twenty colonies were picked up. The genomic DNA of these cells was extracted and analyzed by PCR genotyping and 11 positive clones were identified (Figure 9).

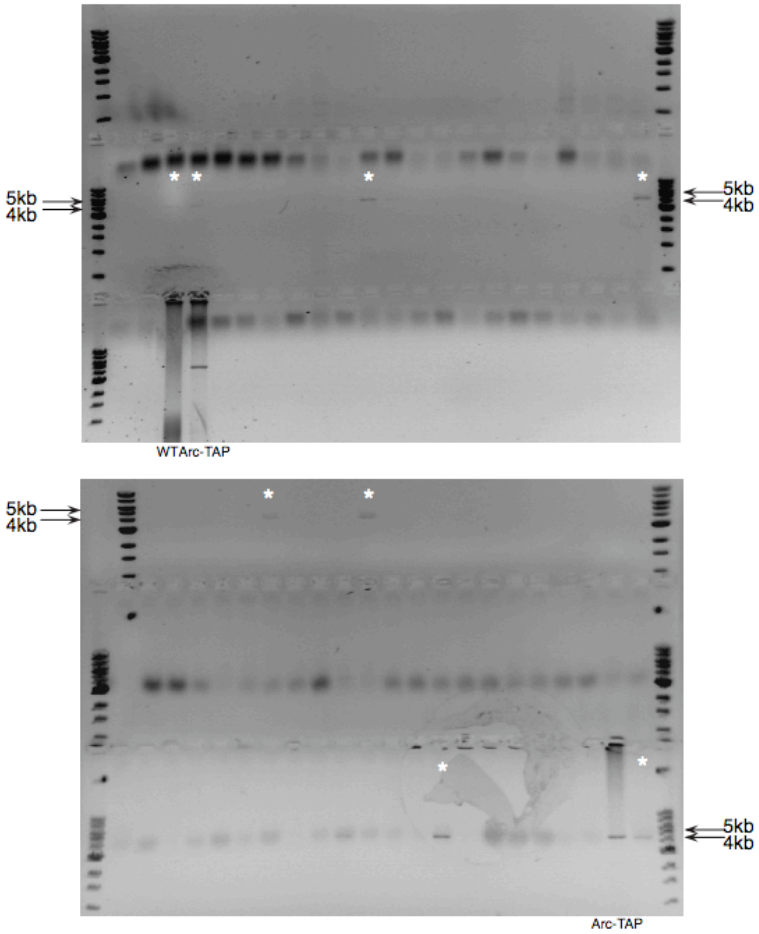

Figure 9. Analysis of Arc-Venus targeted ES cells using polymerase chain reaction (PCR) genotyping. Several ES clones showed the band with expected size of 4625 bp (lanes marked with aster) and are confirmed as correctly targeted Arc-Venus clones.

Discussion

In the initial stage of my project, I generated PSD95-EGFP and Arc-Venus knock-in ES cell lines. By using gene targeting techniques, I inserted two fluorescence tags (EGFP and Venus) in-frame to the 3'end of endogenous genes (PSD-95 and Arc). We chose to utilize gene-targeting approach to fluorescently label the candidate protein, rather than using transgenic methods such as BAC trangenesis or virus-mediated gene transfer, because the in-frame fusion of fluorescent tag is not only capable of recapitulating physiological expression level of the endogenous protein, but also allows convenient observation of its natural dynamics over different time scale. In addition, with the genetically labeled protein, we could accurately define its subcellular localization, thus avoid the cross-reactivity problem of using antibodies especially against close paralogs. Moreover, by utilizing this modular cloning frame-work, we will be able to efficiently replace multiple fluorescent cassettes that are tagging genes of interest.

An *in vitro* ES cell differentiation protocol that induces the formation of WT and PSD95-EGFP ES cells derived neurons (ESNs) was performed and live cell imaging data showed that the PSD95-EGFP fusion protein is stably expressed in differentiated ESNs, suggesting that tagging EGFP with PSD-95 does not alter the cellular expression in the cultured neurons. Next, I carried out immunocytochemistry experiments using antibodies that specifically label dendrite, pre-synaptic and post-synaptic compartments to analyze the synaptic localization of PSD95-EGFP in ESNs. I found that PSD95-EGFP is localized to the postsynaptic side of synapses. This result demonstrates that the replacement of endogenous protein with PSD95-EGFP does not affect its postsynaptic localization in neurons. Overall, these data indicate that EGFP fusion protein is a reliable marker for monitoring endogenous protein, thus validate our experimental approaches. Since generating a knock-in mouse remains relatively inefficient (usually taking several months), this short-term *in vitro* ESN protocol provides a rapid and effective assay for characterizing targeted gene. Hence this generic method could be implemented in the future work of my project. The PSD95-EGFP expression and its subcellular distribution in cultured ESNs suggests that I will be able to

observe the *in vivo* PSD95-EGFP expression within the knock-in mouse of this fluorescently tagged gene.

Upon a closer examination of the immunofluorescent images, I found that PSD95-EGFP fluorescent puncta, which are well contrast with diffuse background fluorescent signals, are present on the process immunoreactive for MAP2 (Figure 8B, C and D). This result indicates that PSD95-EGFP puncta localize along the dendrite and neurite in cultured neurons, which is consistent with the previous report (El-Husseini, Schnell et al. 2000). Functional pre-synaptic sites were further identified in ESNs using anti-synaptophysin antibody (Fletcher, Cameron et al. 1991) (Figure 8B). My result showed that the close appositions of PSD95-EGFP with synaptophysin were only presented in a fraction of synapses, suggesting that PSD95-EGFP might not necessarily localize to the sites that are appose to functional pre-synapses. These data, however, appeared to be in contrast with the previous report that overexpression of PSD-95 enhances pre-synaptic development (El-Husseini, Schnell et al. 2000). The discrepancy between our results and other observers could be possibly due to the non-endogenous expression levels of PSD-95 in these studies. Despite a quantitative measurement is yet required to determine how many PSD95-EGFP-positive puncta represent the functional synaptic sites, our results suggest that under the physiological condition, PSD-95 displays a differential expression pattern within different individual synapses.

It has been known that SAP-102 is highly expressed during early synaptogenesis, whereas PSD-95 seems to dominate in mature synapses. Another recent study found that SAP-102 and PSD-95 play distinct roles in the trafficking of glutamate receptors during synapse development (Elias, Elias et al. 2008). Consistent with those findings, my result from immunostaining with EGFP and SAP-102 also showed that their colocalization appeared only in some of the synapses (Figure 8C), suggesting that a molecular heterogeneity (specifically between PSD-95 and SAP-102) in synapses may exist. In the last series of immunocytochemical experiments, I analyzed the postsynaptic localization of PSD95-EGFP and GluR1. Similar to PSD95-EGFP and SAP-102 staining pattern, colocalization of EGFP and GluR1 is only presented in some synapses. In addition, I found that some synapses

exclusively displayed GluR1 staining, whereas others only showed GFP-positive staining. This result is in agreement with the previous publication, in which PSD-95 KO mice are reported to have no apparent changes in AMPAR function, suggesting that PSD-95 may not be necessary for the recruitment of AMPAR (Beique, Lin et al. 2006). Nevertheless, another possible explanation of the differential co-staining of PSD95-EGFP with SAP-102 and GluR1 could be due to the incapacity of our antibodies for detecting candidate proteins. Overall, these results are consistent with proposed hypothesis that each individual synapse is unique and there exists a high degree of molecular heterogeneity onto a single postsynaptic site (Craig and Boudin 2001). Therefore, it is reasonable to propose that the diversity of scaffolding protein may be tightly correlated with this heterogeneity in single synapse.

Previous studies have shown that the PSD architecture is highly dynamic due to the changes during the process of synaptogenesis and plasticity changes. Although it appears that the numbers of NMDA receptor and PSD-95 are largely fixed in mature neurons, recent studies have implied that a rapid trafficking and reversible insertion of AMPA receptors into the membrane regulated by MAGUK scaffolding proteins occurs in response to neuronal activity (Elias, Elias et al. 2008). Therefore, future work by applying real-time confocal microscopy techniques, such as FRAP (Fluorescence Recovery After Photobleaching) techniques, is required for direct visualization of the natural dynamic behavior of each individual tagged proteins as well as the correlations between different MAGUKs. In addition, the imaging approach can also be combined with pharmacological treatment or RNAi-mediated gene knockdown experiments to elucidate the signaling mechanisms that control activity-dependent dynamics of these MAGUK proteins.

Future Work

During the first stage of my PhD project, I have so far developed PSD95-EGFP and Arc-Venus targeted ES clones. The PSD95-EGFP targeted ES cells have been injected into the blastocysts and five chimeric mice were subsequently created. By performing the *in vitro* differentiation assay to induce targeted ES cells into neurons (ESNs), I showed that the PSD95-EGFP stably expressed in the cultured neurons and inserting the fluorescent tag does not alter the postsynaptic localization of the endogenous protein, thus validate the experimental approach of my project. Molecular cloning work by applying a similar strategy to generate PSD93-mCER and SAP102-mKO targeted ES cells have begun and the targeting constructs will be prepared soon.

In the near future, I will continue to develop PSD93-mCER (mCER: monomeric Cerulean blue) and SAP102-mKO (mKO: monomeric Kusabira Orange) targeted ES clones. Once these clones were established, I will carry on inducing the ES cells into ESNs by applying the well-established differentiation protocol and characterize the fusion protein expressions *in vitro*. To further investigate the molecular heterogeneity in single synapse, a second round of gene targeting in engineered ES cells will be performed. This work aims at inserting a different fluorescent tag into a second gene locus. As a result, the double-targeted ES clones bearing two different fluorescent-tagged genes will be generated. These ES cell lines would become a useful tool to observe the static subcellular distribution of the tagged molecule within individual synapse. By utilizing a variety of imaging techniques, such as FRAP and real-time imaging, I will also study the dynamics of these tagged molecules. Further more, imaging techniques will be combined with pharmacological manipulations (such as TTX, MK801 and AP5) as well as the RNAi-mediated gene knockdown in the neuronal cultures to further dissect the signaling pathway in the PSD complex. Arc-Venus targeted clones will be characterized by using the same strategy. Cultured neurons expressing Arc-Venus can be subjected to various RNAi experiments, in particular with PSD-95 depletion, to further identify the regulatory roles of Arc and PSD-95 during the activity-dependent AMPAR trafficking process.

In the long-term, I will complete the generation of four MAGUK genes fused with fluorescent tags, including PSD95-EGFP, PSD93-mCER, SAP102-mKO, and Arc-Venus knockin mice. After these mice were produced, neuronal cells will be dissociated and subjected to the in-depth functional imaging experiments. These fluorescently tagged mice will also be used to generate double knock-in mice (i.e. PSD95-EGFP mice and SAP102-mKO mice) in which multiple tagged synaptic proteins can be observed simultaneously.

An overview of the project timeline incorporating the key activities is listed in Table 1.

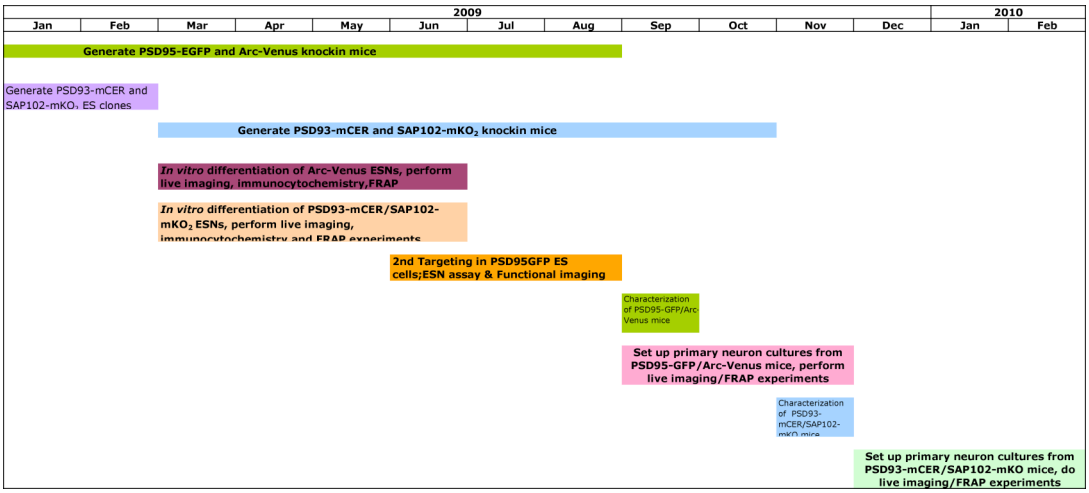

Table 1. Overview of the project future work of 2009 to early 2010.

Reference:

Beique, J. C., D. T. Lin, et al. (2006). "Synapse-specific regulation of AMPA receptor function by PSD-95." Proc Natl Acad Sci U S A **103**(51): 19535-40.

Brenman, J. E., K. S. Christopherson, et al. (1996). "Cloning and characterization of postsynaptic density 93, a nitric oxide synthase interacting protein." J Neurosci **16**(23): 7407-15.

Chowdhury, S., J. D. Shepherd, et al. (2006). "Arc/Arg3.1 interacts with the endocytic machinery to regulate AMPA receptor trafficking." Neuron **52**(3): 445-59.

Craig, A. M. and H. Boudin (2001). "Molecular heterogeneity of central synapses: afferent and target regulation." Nat Neurosci **4**(6): 569-78.

El-Husseini, A. E., E. Schnell, et al. (2000). "PSD-95 involvement in maturation of excitatory synapses." Science **290**(5495): 1364-8.

Elias, G. M., L. A. Elias, et al. (2008). "Differential trafficking of AMPA and NMDA receptors by SAP102 and PSD-95 underlies synapse development." Proc Natl Acad Sci U S A **105**(52): 20953-8.

Emes, R. D., A. J. Pocklington, et al. (2008). "Evolutionary expansion and anatomical specialization of synapse proteome complexity." Nat Neurosci **11**(7): 799-806.

Fletcher, T. L., P. Cameron, et al. (1991). "The distribution of synapsin I and synaptophysin in hippocampal neurons developing in culture." J Neurosci **11**(6): 1617-26.

Fukaya, M., H. Ueda, et al. (1999). "Distinct spatiotemporal expression of mRNAs for the PSD-95/SAP90 protein family in the mouse brain." Neurosci Res **33**(2): 111-8.

Gardoni, F., E. Marcello, et al. (2009). "Postsynaptic density-membrane associated guanylate kinase proteins (PSD-MAGUKs) and their role in CNS disorders." Neuroscience **158**(1): 324-33.

Husi, H., M. A. Ward, et al. (2000). "Proteomic analysis of NMDA receptor-adhesion protein signaling complexes." Nat Neurosci **3**(7): 661-9.

Kennedy, M. B. (2000). "Signal-processing machines at the postsynaptic density." Science **290**(5492): 750-4.

Kim, E., K. O. Cho, et al. (1996). "Heteromultimerization and NMDA receptor-clustering activity of Chapsyn-110, a member of the PSD-95 family of proteins." Neuron **17**(1): 103-13.

Kornau, H. C., L. T. Schenker, et al. (1995). "Domain interaction between NMDA receptor subunits and the postsynaptic density protein PSD-95." Science **269**(5231): 1737-40.

Liu, P., N. A. Jenkins, et al. (2003). "A highly efficient recombineering-based method for generating

conditional knockout mutations." Genome Res **13**(3): 476-84.

Marrs, G. S., S. H. Green, et al. (2001). "Rapid formation and remodeling of postsynaptic densities in developing dendrites." Nat Neurosci **4**(10): 1006-13.

Moga, D. E., M. E. Calhoun, et al. (2004). "Activity-regulated cytoskeletal-associated protein is localized to recently activated excitatory synapses." Neuroscience **125**(1): 7-11.

Muller, B. M., U. Kistner, et al. (1996). "SAP102, a novel postsynaptic protein that interacts with NMDA receptor complexes in vivo." Neuron **17**(2): 255-65.

Niethammer, M., E. Kim, et al. (1996). "Interaction between the C terminus of NMDA receptor subunits and multiple members of the PSD-95 family of membrane-associated guanylate kinases." J Neurosci **16**(7): 2157-63.

Okabe, S., H. D. Kim, et al. (1999). "Continual remodeling of postsynaptic density and its regulation by synaptic activity." Nat Neurosci **2**(9): 804-11.

Plath, N., O. Ohana, et al. (2006). "Arc/Arg3.1 is essential for the consolidation of synaptic plasticity and memories." Neuron **52**(3): 437-44.

Sans, N., R. S. Petralia, et al. (2000). "A developmental change in NMDA receptor-associated proteins at hippocampal synapses." J Neurosci **20**(3): 1260-71.

Schnell, E., M. Sizemore, et al. (2002). "Direct interactions between PSD-95 and stargazin control synaptic AMPA receptor number." Proc Natl Acad Sci U S A **99**(21): 13902-7.

Sheng, M. and M. E. Greenberg (1990). "The regulation and function of c-fos and other immediate early genes in the nervous system." Neuron **4**(4): 477-85.

Stavridis, M. P. and A. G. Smith (2003). "Neural differentiation of mouse embryonic stem cells." Biochem Soc Trans **31**(Pt 1): 45-9.

Steward, O. and P. F. Worley (2001). "A cellular mechanism for targeting newly synthesized mRNAs to synaptic sites on dendrites." Proc Natl Acad Sci U S A **98**(13): 7062-8.

Waltereit, R., B. Dammermann, et al. (2001). "Arg3.1/Arc mRNA induction by Ca2+ and cAMP requires protein kinase A and mitogen-activated protein kinase/extracellular regulated kinase activation." J Neurosci **21**(15): 5484-93.

Yin, Y., G. M. Edelman, et al. (2002). "The brain-derived neurotrophic factor enhances synthesis of Arc in synaptoneurosomes." Proc Natl Acad Sci U S A **99**(4): 2368-73.